EFFECT OF AXIAL LOADS ON RADIAL STRESS IN CURVED BEAMS

Chung K. Cheung and *Harold C. Sorensen*

Graduate Student and Associate Professor
Department of Civil and Environmental Engineering
Washington State University, Pullman, WA 99164

(Received 31 August 1982)

ABSTRACT

Radial tension failures have occurred in some curved glulam beams. Radial stresses in curved beams are generally computed using only the bending moment, e.g., Wilson's equation. This work was performed to provide additional insight into the effect on the radial stresses due to the axial loads that are present in the curved beams.

Equations of tangential, radial, and shear stress were developed for curved beams under an axial load. The theory of elasticity with polar coordinates for plane stress applied to an orthotropic material was used. Two loblolly pine glulam specimens (orthotropic) and one aluminum specimen (isotropic) with sharp radii and high d/R ratios were tested for the purpose of verifying the theoretical tangential and radial stress distributions that were predicted by the equations. In the aluminum specimen test, theoretical and experimental values compare favorably. In the glulam specimen tests, a favorable agreement was obtained for the tangential stress between the theoretical and experimental values, while the experimental radial stress values were about 2 to 4 times larger than the theoretical values.

The theoretical radial stresses predicted by Wilson's equation were verified by a rigorous theory of elasticity solution as both solutions gave almost identical results. Since the elasticity solution included the effect of axial load, we conclude that the effect of axial load on the radial stress in curved beams is small.

Keywords: Axial loads, beams, radial stress.

INTRODUCTION

Radial-tension separation is a problem that exists when using curved glulam structural members. These separations have not caused structural collapse, but there have been instances where radially fractured members have been removed and/or repaired. Restoration is costly.

The causes of radial stress in glulam curved beams have not yet been fully understood. The factors that have been considered in stress determination and analysis are the effect of the bending moment, shrinkage and swelling of the wood, and the springback tendency due to the bending of the laminations.

In the stress analysis of curved beams, the effect of an axial load on the radial stress has generally been ignored, while the effects of bending moment and axial load have been superimposed for the tangential (circumferential) stress. This oversight could be critical in wood because the allowable tension stress perpendicular to the grain is 1.8% to 12% of the allowable tension stress parallel to the grain.

The purpose of this paper is to call attention to the effect of axial loads in the design of glulam curved beams. The study consists of two parts. The first part deals with formula development where a set of stress equations (tangential, radial, and shear) are developed by using the theory of elasticity applied to an orthotropic material under an axial load. The second part consists of experimental tests that are used to verify the theoretical results. Two glulam specimens and one alumi-

Wood and Fiber Science, 15(3), 1983, pp. 263–275

num specimen were tested to observe the stress correlation between the theory and the experimental tests.

Symbols

a = radius of curvature at the concave surface
b = radius of curvature at the convex surface
d = height of the rectangular cross section
t = width of the rectangular cross section
R = radius of curvature of the centroid of the cross section
Y = distance away from the centroid of the cross section
r = radius in polar coordinates system
θ = angle in polar coordinates system
c_1, c_2, c_3, c_4 = material property constants
B, C, D; $\bar{B}, \bar{C}, \bar{D}$ = geometrical parameters
m_3, m_4; $\bar{m}_3, \bar{m}_4$ = roots of characteristic equations
N_p, N_m = determinant of matrices
M = applied bending moment
V = applied shear force
P = applied axial load
$\sigma_{\theta_1}, \sigma_{\theta_2}, \sigma_\theta$ = tangential stresses
$\sigma_{r_1}, \sigma_{r_2}, \sigma_r$ = radial stresses
$\tau_{r\theta_1}, \tau_{r\theta_2}, \tau_{r\theta}$ = shear stresses
E, G, μ = modulus of elasticity, modulus of rigidity and Poisson's ratio of isotropic materials
E_i, E_j = moduli of elasticity in the i and j direction, respectively
E_θ, E_r = moduli of elasticity in the tangential and radial direction, respectively
E_L, E_R = moduli of elasticity of wood in the longitudinal and radial direction, respectively
$G_{r\theta}$ = modulus of shear in the r-θ plane
G_{LR} = modulus of shear of wood in the L-R plane
$\mu_{\theta r}$ = Poisson's ratio (ratio of strains in the r direction to θ direction (for a uniform normal stress in the θ direction))
μ_{ij}, μ_{ji} = Poisson's ratio as defined in $\mu_{\theta r}$
μ_{LR} = Poisson's ratio for wood as defined in $\mu_{\theta r}$
$\phi_{(r,\theta)}, \phi_1, \phi_2, \phi$ = stress functions
$f_1(r), f_2(r)$ = functions of r

LITERATURE REVIEW

The Winkler-Bach solution is a well-known approximate solution for curved members, which provides the tangential stress distribution for bending. Exact solutions for tangential, radial, and shear stress for curved beams under bending and shear loads are provided by Timoshenko and Goodier (1951). Oden (1967) used the equations of equilibrium to develop a set of stress equations that allow

for pressure on the circular boundary, axial force, and bending moment. All of these formulas were developed to determine stresses in curved beams made from isotropic materials.

Wood is an orthotropic material with different elastic properties along three mutually perpendicular axes. Therefore, all of the existing equations were considered questionable when applied to glulam curved beam design. It is especially important to recognize that in general wood is weak in tension in the direction perpendicular to the grain.

Wilson (1939) developed a simple and conservative equation for radial stress distribution, which is recommended by the American Institute of Timber Construction (A.I.T.C.). This radial stress equation is

$$\sigma_r = \frac{3}{2}\left(\frac{M}{bd(R + Y)}\right)\left(1 - \frac{Y}{(d/2)^2}\right) \tag{a}$$

Norris (1963) developed the first rigorous solution for analyzing wood curved beams under bending by using the theory of elasticity applied to orthotropic materials. Following the same trend as Norris, Foschi (1968) extended the exact solution for all load combinations of bending, shear, and axial force. Although the exact solution was provided, it was not commonly used in design or analysis. The reasons are the complexity of the solution and the lack of known elastic properties for different wood species.

FORMULA DEVELOPMENT

Polar coordinates were used throughout the formula development. Without repeating all of the basic elasticity equations, the main steps of the development will be shown.

The equation of equilibrium is satisfied by taking a stress function $\phi_{(r,\theta)}$ which expresses the stresses as follows:

$$\sigma_r = \frac{1}{r}\frac{\partial \phi}{\partial r} + \frac{1}{r^2}\frac{\partial^2 \phi}{\partial \theta^2} \tag{1}$$

$$\sigma_\theta = \frac{\partial^2 \phi}{\partial r^2} \tag{2}$$

$$\tau_{r\theta} = \frac{1}{r^2}\frac{\partial \phi}{\partial \theta} - \frac{1}{r}\frac{\partial^2 \phi}{\partial r\, \partial \theta} \tag{3}$$

The compatibility equation of deformation is obtained by eliminating the displacement terms in the strain-displacement equation. The elastic property constants relationship for an orthotropic material is

$$\frac{\mu_{ij}}{E_i} = \frac{\mu_{ji}}{E_j} \tag{4}$$

Equation 4 is substituted into the stress-strain equations and then substituted into the compatibility equation. In terms of the stress function $\phi_{(r,\theta)}$, the compatibility equation becomes

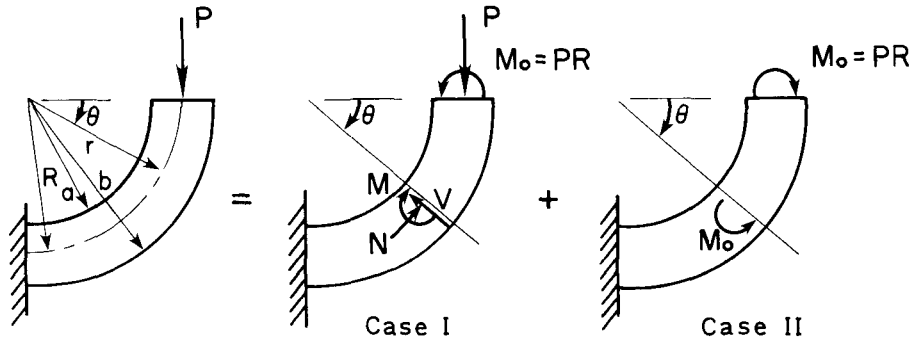

FIG. 1. Cantilever curved beam model.

$$c_1\frac{\partial^4\phi}{\partial r^4} + 2c_1\frac{1}{r}\frac{\partial^3\phi}{\partial r^3} - c_2\frac{1}{r^2}\frac{\partial^2\phi}{\partial r^2} + c_2\frac{1}{r^3}\frac{\partial\phi}{\partial r} + (2c_2 - c_3)\frac{1}{r^4}\frac{\partial^2\phi}{\partial\theta^2} + c_3\frac{1}{r^3}\frac{\partial^3}{\partial\theta^2\,\partial r} - c_3\frac{1}{r^2}\frac{\partial^4}{\partial\theta^2\,\partial r^2} + c_2\frac{1}{r^4}\frac{\partial^4\phi}{\partial\theta^4} = 0 \tag{5}$$

where

$$c_1 = \frac{1}{E_\theta}$$
$$c_2 = \frac{1}{E_r}$$
$$c_3 = 2\frac{\mu_{\theta r}}{E_\theta} - \frac{1}{G_{r\theta}} \tag{5.1}$$
$$c_4 = \frac{1}{E_r} - 2\frac{\mu_{\theta r}}{E_\theta} + \frac{1}{G_{r\theta}}$$

In establishing the solution by using simple stress functions, the problem is separated into two parts (Fig. 1).

The stress function for Case I is

$$\phi_1 = f_1(r)\cos\theta \tag{6}$$

The reason for using a cosine function is that both the normal force N and bending moment M along the curve vary as a cosine function. By substituting the stress function ϕ_1 into Eqs. 1 and 2, both resultant tangential and radial stresses, σ_t and σ_r, are also cosine functions. The same principle applies to the shear stress. Similar reasoning can be applied to all three of the stresses in Case II.

The stress function for Case II is

$$\phi_2 = f_2(r) \tag{7}$$

Upon substitution of both stress functions into the compatibility Eq. 5, two homogeneous linear differential equations were obtained. These equations were solved by letting $f(r) = r^m$. Then the corresponding characteristic equations were solved. Unknown constants in these solutions were determined by using boundary conditions (BC) as follows:

BC #1 $$\sigma_r = \tau_{r\theta} = 0 \quad \text{for} \quad r = a \quad \text{and} \quad r = b \tag{8}$$

BC #2 $$\int_a^b \sigma_\theta \, dr = -P \quad \text{at} \quad \theta = 0^\circ \tag{9}$$

BC #3 $$\int_a^b \sigma_\theta r \, dr = -M_0 \tag{10}$$

BC #1 and BC #2 were applied to Case I and BC #1 and BC #3 were applied to Case II. The stress distribution equations for Case I are:

$$\sigma_{r,1} = \left[\frac{B}{r} + C(m_3 - 1)r^{m_3-2} + D(m_4 - 1)r^{m_4-2}\right]\cos\theta \tag{11}$$

$$\sigma_{\theta,1} = \left[\frac{B}{r} + Cm_3(m_3 - 1)r^{m_3-2} + Dm_4(m_4 - 1)r^{m_4-2}\right]\cos\theta \tag{12}$$

$$\tau_{r\theta,1} = \left[\frac{B}{r} + C(m_3 - 1)r^{m_3-2} + D(m_4 - 1)r^{m_4-2}\right]\sin\theta \tag{13}$$

where
$$B = \left(\frac{P}{N_p}\right)(m_3 - 1)(m_4 - 1)(a^{m_4-1}b^{m_3-1} - a^{m_3-1}b^{m_4-1})$$
$$C = \left(\frac{P}{N_p}\right)(m_4 - 1)(b^{m_4-1} - a^{m_4-1}) \tag{13.1}$$
$$D = \left(\frac{P}{N_p}\right)(m_3 - 1)(a^{m_3-1} - b^{m_3-1})$$
$$N_p = (m_3 - m_4)(b^{m_4-1} - a^{m_4-1})(b^{m_3-1} - a^{m_3-1}) + \left[\ln\left(\frac{b}{a}\right)\right](m_3 - 1)(m_4 - 1)(a^{m_3-1}b^{m_4-1} - a^{m_4-1}b^{m_3-1}) \tag{13.2}$$

$$m_3 = 1 + \sqrt{1 + \frac{c_4}{c_1}} \qquad m_4 = 1 - \sqrt{1 + \frac{c_4}{c_1}} \tag{13.3}$$

Similarly the stress equations for Case II are:

$$\sigma_{r,2} = 2\bar{B} + \bar{C}\bar{m}_3 r^{\bar{m}_3-2} + \bar{D}\bar{m}_4 r^{\bar{m}_4-2} \tag{14}$$

$$\sigma_{\theta,2} = 2\bar{B} + \bar{C}\bar{m}_3(\bar{m}_3 - 1)r^{\bar{m}_3-2} + \bar{D}\bar{m}_4(\bar{m}_4 - 1)r^{\bar{m}_4-2} \tag{15}$$

$$\tau_{r\theta,2} = 0 \tag{16}$$

where
$$\bar{B} = \left(\frac{M}{N_m}\right)\bar{m}_3\bar{m}_4(a^{\bar{m}_3}b^{\bar{m}_4} - a^{\bar{m}_4}b^{\bar{m}_3})$$
$$\bar{C} = \left(\frac{M}{N_m}\right)2\bar{m}_4(a^{\bar{m}_4}b^2 - a^2b^{\bar{m}_4}) \tag{16.1}$$
$$\bar{D} = \left(\frac{M}{N_m}\right)2\bar{m}_3(a^2b^{\bar{m}_3} - a^{\bar{m}_3}b^2)$$
$$N_m = 2\bar{m}_3(b^{\bar{m}_4} - a^{\bar{m}_4})(a^2b^{\bar{m}_3} - a^{\bar{m}_3}b^2) + 2\bar{m}_4(b^{\bar{m}_3} - a^{\bar{m}_3})(a^{\bar{m}_4}b^2 - a^2b^{\bar{m}_4}) + \bar{m}_3\bar{m}_4(b^2 - a^2)(a^{\bar{m}_3}b^{\bar{m}_4} - a^{\bar{m}_4}b^{\bar{m}_3}) \tag{16.2}$$

$$\bar{m}_3 = 1 + \sqrt{\frac{c_2}{c_1}}$$

$$\bar{m}_4 = 1 - \sqrt{\frac{c_2}{c_1}} \tag{16.3}$$

$$M = P\left(\frac{a + b}{2}\right)$$

The resulting equations for an axial load on a curved beam are:

$$\sigma_r = \left[\frac{B}{r} + C(m_3 - 1)r^{m_3-2} + D(m_4 - 1)r^{m_4-2}\right]\cos\theta + 2\bar{B} + \bar{C}\bar{m}_3 r^{\bar{m}_3-2} + \bar{D}\bar{m}_4 r^{\bar{m}_4-2} \tag{17}$$

$$\sigma_\theta = \left[\frac{B}{r} + Cm_3(m_3 - 1)r^{m_3-2} + Dm_4(m_4 - 1)r^{m_4-2}\right]\cos\theta + 2\bar{B} + \bar{C}\bar{m}_3(\bar{m}_3 - 1)r^{\bar{m}_3-2} + \bar{D}\bar{m}_4(\bar{m}_4 - 1)r^{\bar{m}_4-2} \tag{18}$$

$$\tau_{r\theta} = \left[\frac{B}{r} + C(m_3 - 1)r^{m_3-2} + D(m_4 - 1)r^{m_4-2}\right]\sin\theta \tag{19}$$

APPLICATION OF THE SOLUTION

The stress equations 17, 18, and 19 were developed for a constant narrow rectangular cross-sectional curved beam with a unit cross-sectional width. The stress distributions for an orthotropic (loblolly pine) cantilever curved beam with a unit force at the end section were calculated to demonstrate the solution. The calculations were then repeated for an isotropic material. Both sets of stress distributions are shown in Fig. 2. Values inside and outside the parentheses in Fig. 2 apply to an orthotropic material (loblolly pine) and an isotropic material, respectively (see Appendix I). The solution shown for an isotropic material is valid for any isotropic material.

EXPERIMENTAL TEST—MATERIALS AND METHODS

An (2024-T351) aluminum (an isotropic material) curved beam (Fig. 3) with d/R = 1.33 and two 41-laminas loblolly pine glulam (an orthotropic material) beams (Fig. 4) with d/R = 0.39 were tested to observe the strain distribution. These sharp radius, high d/R specimens were tested in order to produce radial stresses large enough to be accurately measured. Electric strain gauges were used to measure the strains. On the aluminum specimen, 120 degree rosette gauges were used to obtain the experimental strains. These values were substituted into Hooke's law to obtain the experimental radial and tangential stresses. On the glulam specimen, strain gauges oriented directly in the radial and tangential directions were used to obtain the strains, which were then converted to experimental stresses through Hooke's law for an orthotropic material. The resulting experimental stress distributions were plotted along with the theoretical values in Figures 5–7. The theoretical stress distributions were determined with a (Fortran IV) computer program as described in Appendix II. In the glulam specimen pulling load test, visible separation along the glue line occurred when the load reached 470 pounds.

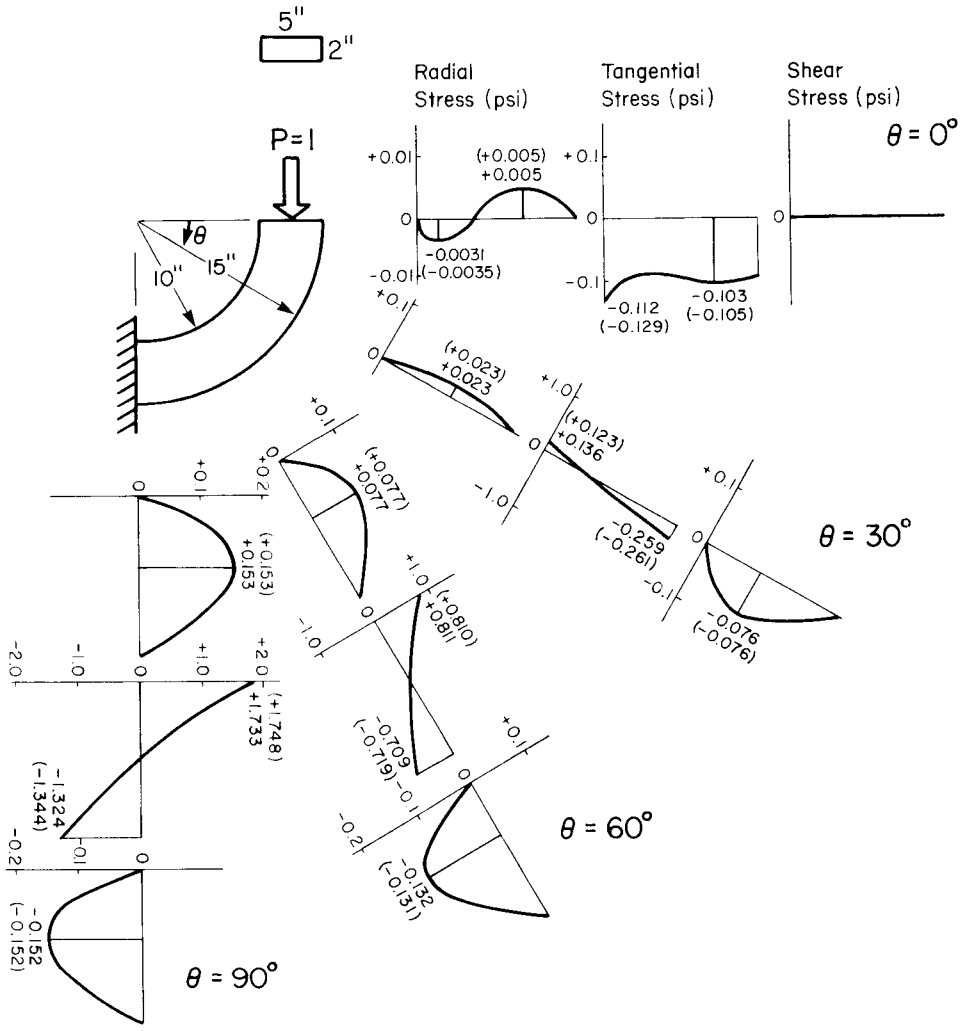

FIG. 2. Stress distribution plots for the example solution. (Values inside the parentheses are for the orthotropic material (loblolly pine), while values outside the parentheses are for the isotropic material.)

DISCUSSION

Considering the stress distributions for the example (Fig. 2), a pure axial load at a radial cross section of a curved beam produces a very small effect in the stress at the location of the load, but the stress increases with increasing distance from the loaded section. In comparing the resulting theoretical stress value in Fig. 2, a negligible difference of radial stress was found between the orthotropic material (loblolly pine) and the isotropic material. The isotropic material stress formulas are applied to wood, although only the loblolly pine was used as an orthotropic material model in the example.

The aluminum specimen (an isotropic material) test results reflected an agree-

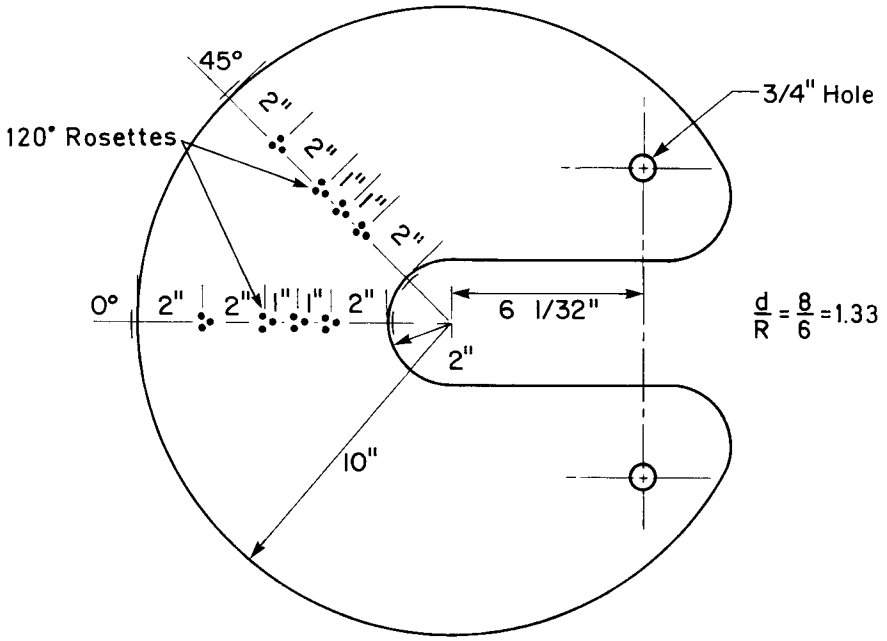

FIG. 3. The dimensions and locations of strain gauges for the aluminum specimen.

ment between the theoretical and experimental values of tangential and radial stress as shown in Fig. 5.

The loblolly pine glulam specimen test used to verify the formula for an orthotropic material showed favorable agreement in the tangential stress between the theoretical and experimental values as shown in Figs. 6 and 7. However, the experimental radial stress values were about 1.2 to 2 times the theoretical values at the center sections and 0.5 to 4 at the 45 degree sections as shown in Figs. 6 and 7. These discrepancies may be due to the following reason. No elastic prop-

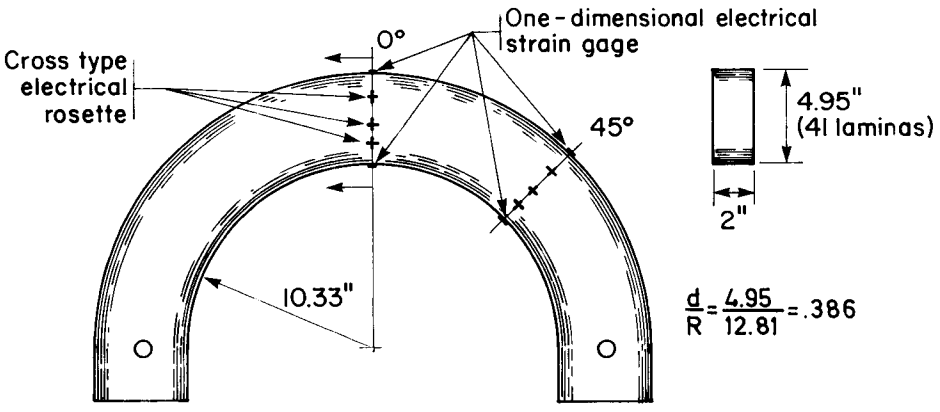

FIG. 4. The dimensions and locations of strain gauges for the glulam specimens.

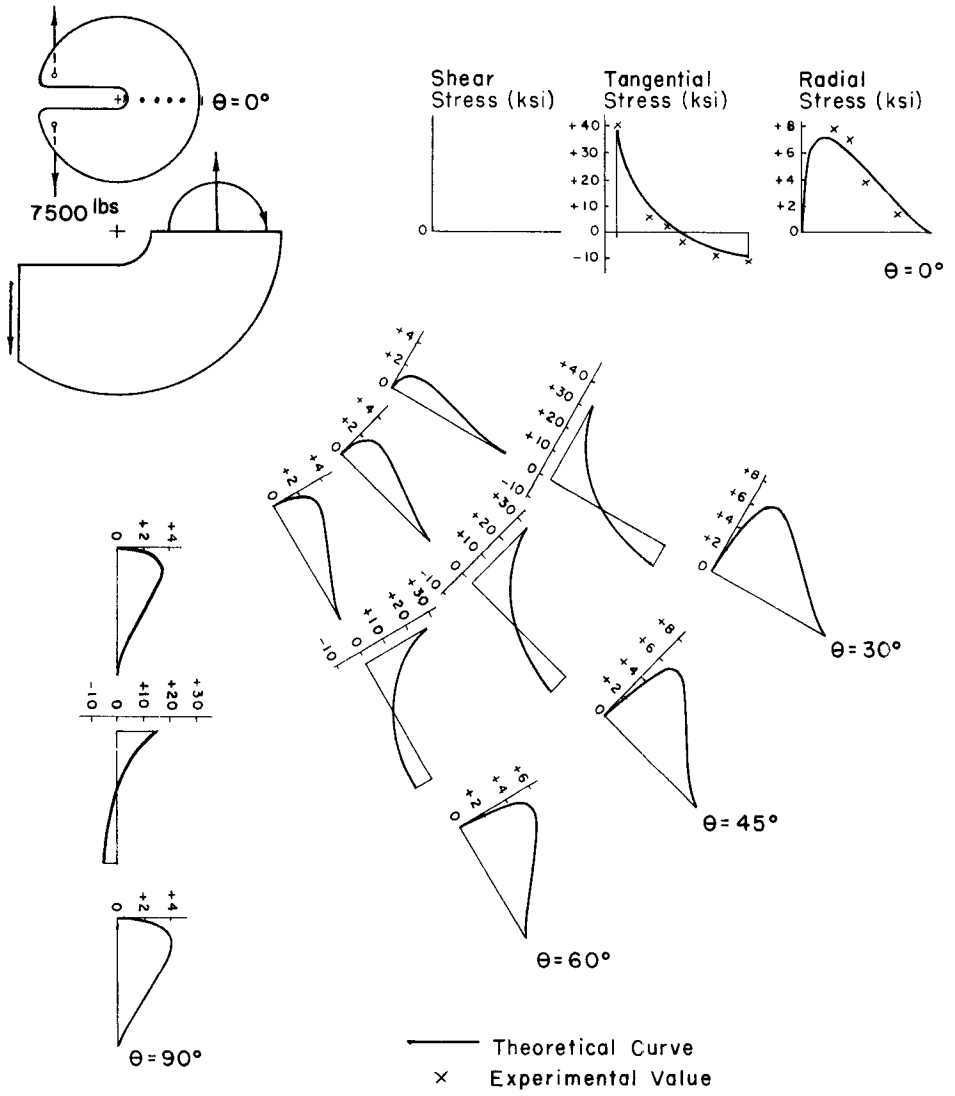

FIG. 5. Distributions of theoretical stress and experimental stress for the aluminum specimen pulling test.

erty parameter test was performed, and the parameters used were picked from the common engineering table. This appears to be a very important source of error. Past research by others indicates that accurate E_R values for all laminations are absolutely essential.

Wilson's design equation (Eq. a in Literature Review) was used to plot the radial stress distribution for comparison with the theoretical and experimental radial stress values. The maximum radial stress values of the theoretical curve developed in this paper and Wilson's equation were almost identical as shown in Figs. 6 and 7, which confirms the agreement between Wilson's equation and the

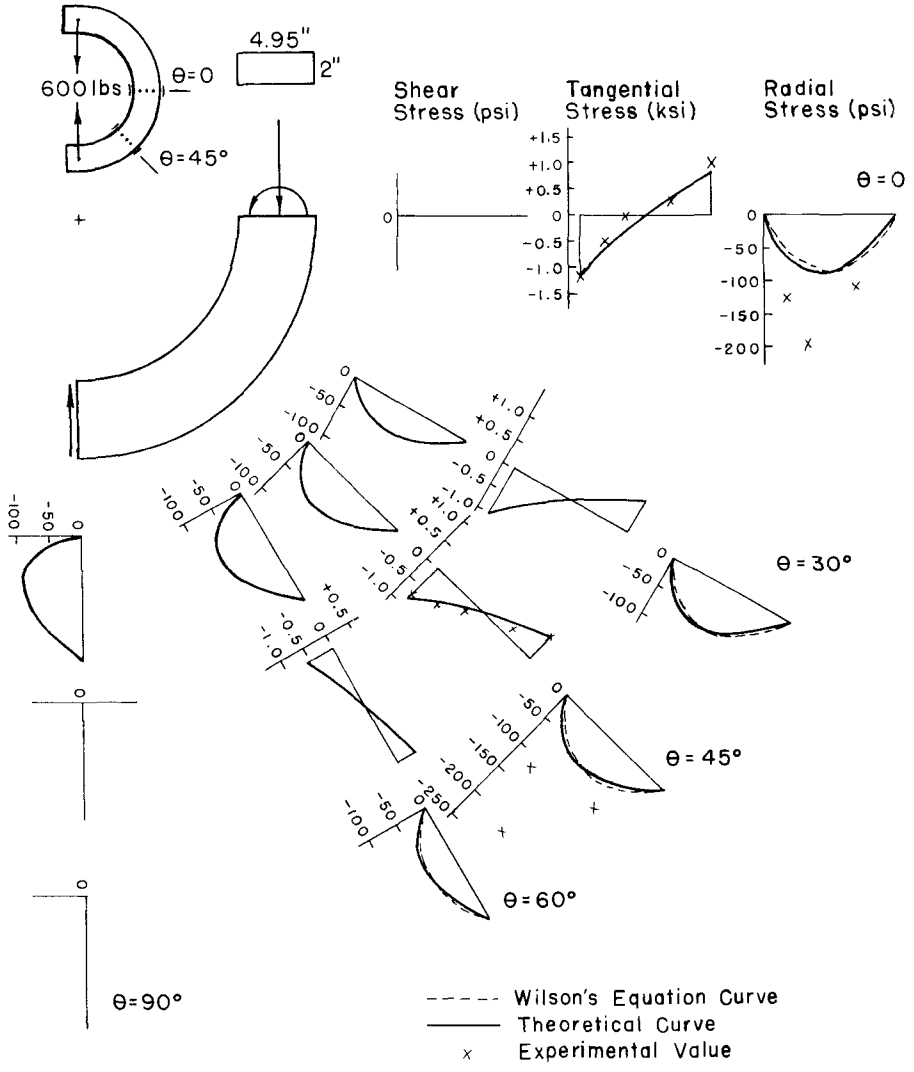

FIG. 6. Distributions of theoretical stress and experimental stress for the glulam specimen pushing load test.

theory of elasticity for an included angle of 180 degrees. This agreement indicates that the effect of P is small and reinforces the use of Wilson's equation for design.

The actual radial stress exceeded the predicted stress by a factor as high as 4 for these sharp radius beams. Therefore judgment must be exercised in applying the design stress equation to obtain the predicted stress or an additional safety factor must be applied to the 5% exclusion limit value for tension perpendicular to the grain as given in the design table.

SUMMARY AND CONCLUSION

An exact solution for an axial load on a curved beam was developed by using the theory of elasticity with polar coordinates for a plane stress problem applied

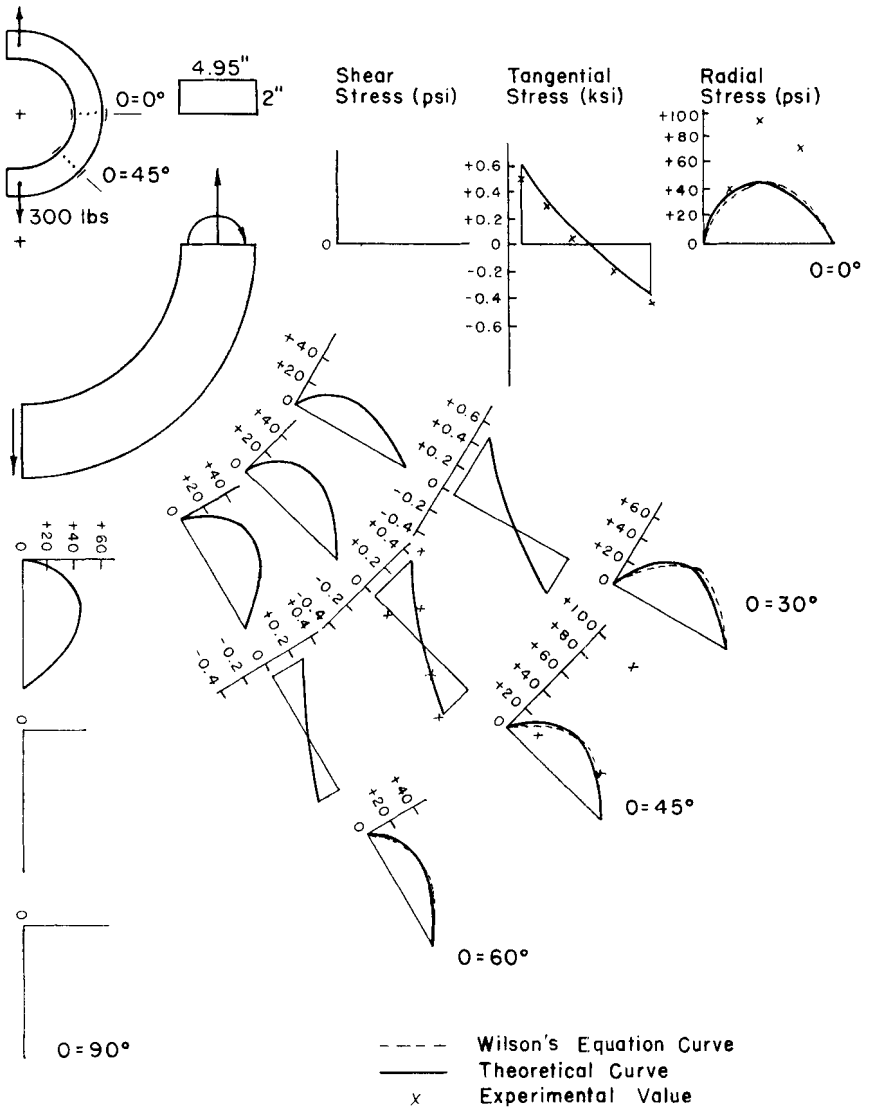

FIG. 7. Distributions of theoretical stress and experimental stress for the glulam specimen pulling load test.

to an orthotropic material. An aluminum specimen pulling load test had been performed to verify the theoretical tangential and radial stress distributions. A good agreement was obtained between the experimental and the theoretical stress values for this aluminum specimen test.

Two glulam curved timber specimens were tested with pulling and pushing loads to verify the theoretical radial and tangential stress values. These glulam specimen tests yielded experimental values of tangential stress which compared favorably to the theoretical stress values. The values of the radial stress were about 2 to 4 times larger than the theoretical stress values. The maximum radial stress values

for the theoretical curve developed in this paper and Wilson's design equation curve were almost identical. Further studies of glulam curved beams are needed in the areas concerning residual tension separation and solutions for external loads other than bending moment, shear, and axial force at the end section.

REFERENCES

AMERICAN INSTITUTE OF TIMBER CONSTRUCTION. 1966. Timber construction manual. 1st ed., John Wiley and Sons, N.Y.

AMERICAN SOCIETY OF CIVIL ENGINEERS. 1975. A design guide and commentary—Wood structures.

FOSCHI, R. O. 1968. Plane-stress problem in a body with cylindrical anisotropy with special reference to curved Douglas-fir beams. Dep. Publ. No. 1244, Dep. Forest Rural Development, Ottawa, Ontario.

FOX, S. P. 1970. Experimental verification of a stress analysis method for the double-tapered pitched glued-laminated beam. Dep. Publ. No. 1277, Department of Fisheries and Forestry, Canadian Forest Service, Vancouver, B.C., Canada.

NORRIS, C. B. 1963. Stress within curved laminated beams of Douglas-fir. FPL-20, Forest Prod. Lab., Madison, WI.

ODEN, T. J. 1967. Mechanics of elastic structures. McGraw-Hill, N.Y.

TIMOSHENKO, S., AND J. N. GOODIER. 1951. Theory of elasticity. 2nd ed., McGraw-Hill, N.Y. Pp. 83–88.

WILSON, T. R. C. 1939. The glued-laminated wooden arch. Technical Bulletin No. 691, USDA. Washington D.C. Pp. 118–119.

ZAHN, JOHN J. 1969. Residual stress in curved laminated beam. J. of Structures Div., Proc. of the American Society of Civil Engineers, 95 (ST 12). Pp. 2873–2890.

APPENDIX I

In order to show the stress distributions in an orthotropic (or isotropic) cantilever curved beam, the following problem was solved using the dimensions a = 10″, b = 15″, t = 2″. A unit axial force acts at the end section. Because the cross-sectional width t is no longer unity, all the resultant stress values have to be divided by t. To represent an orthotropic material model, loblolly pine was used. The elastic parameters corresponding to 13.4% moisture content and 0.465 g/cm^3 density are:

$$E_L = 1608.0 \times 10^3 \text{ psi}$$
$$E_R = 181.8 \times 10^3 \text{ psi}$$
$$G_{LR} = 131.0 \times 10^3 \text{ psi}$$
$$\mu_{LR} = 0.328$$

Then, the stress equations 17, 18, and 19 were solved using these dimensions and elastic property parameters. Because a large number of calculations were required, a (Fortran IV) computer program (Appendix II) was used to provide all the values required to plot the stress distributions at the 0°, 30°, 45°, and 60° sections which are shown in Fig. 2 (values inside the parentheses).

For isotropic materials, the elastic property parameter relationships $G = E/2(1 + \mu)$ and $E_L = E_R = E$ were applied to yield the values of the roots ($m_3 = 3$, $m_4 = -1$, and $\bar{m}_3 = 2$, $\bar{m}_4 = 0$), and the stress equations were simplified. Because m_3, m_4 and $\bar{m}_3$, $\bar{m}_4$ are defined, the elastic property parameters of an isotropic material are not needed in using Eqs. 17, 18, and 19 to determine the stresses. For a comparison of resultant stresses between an orthotropic material and an isotropic material, the previous example was solved again as an isotropic material. The resultant stresses were plotted in Fig. 2 (values outside the parentheses).

APPENDIX II

A (Fortran IV) computer program was written to perform the calculations for the example plots and the theoretical curve plots. This program contains the basic steps as follows:

1. input data—elastic property parameters (E_L, E_R, G_{LR}, μ_{LR}), inner and outer radii (a, b), thickness (t), external loading (moment M and normal force N at the end section)
2. determine c_1, c_2, and c_4 by Eq. 5.1
3. determine m_3, m_4 and $\bar{m}_3$, $\bar{m}_4$ by Eqs. 13.3 and 16.3
4. determine N_M and N_P by Eqs. 13.2 and 16.2
5. determine σ_r, σ_θ, $\tau_{r\theta}$ by Eqs. 17, 18, and 19.

The stresses σ_r, σ_θ and $\tau_{r\theta}$ due to an axial force with the corresponding moment (Case I) and pure moment (Case II) are determined separately. This computer program can be used to perform the calculations for any combination of bending moment and normal force acting at the end section. The output consists of the stress values at the 1/10 points along the cross section at the 0°, 30°, 45°, 60°, and 90° sections along the circular curve.